Journal Name

Dynamic Article Links ►

ARTICLE TYPE

Combining oxime-based [Mn_6] clusters with cyanometalates: 1D chains of [Mn_6] SMMs from [$M(CN_2)]^-$ (M= Au, Ag)

Sergio Sanz,[a] Jamie M. Frost,[a] Giulia Lorusso,[b] Marco Evangelisti,[b] Mateusz B. Pitak,[c] Simon J. Coles,[c] Gary S. Nichol[a] and Euan K. Brechin*[a]

Received (in XXX, XXX) Xth XXXXXXXXX 20XX, Accepted Xth XXXXXXXXX 20XX
DOI:

The linear [$M(CN)_2]^-$ (M= Au, Ag) anions can be used as metalloligands in oxime-based Mn chemistry to afford 1D chains of [Mn^{III}_6] Single-Molecule Magnets (SMMs).

Supramolecular assemblies are multicomponent systems in which molecular units, or building blocks, are assembled into various architectures in 0-3D.[1] With the realisation that intermolecular interactions may play an important, non-innocent role in influencing the properties of molecules, synthetic chemists have successfully devised multiple strategies to construct such discrete or polymeric materials, harnessing different types of interactions, from simple coordination-driven self-assembly to hydrogen bonding and π- π stacking.[2] Design is often driven by the demand for multifunctional materials with tuneable magnetic, conducting or optical properties.[3] Assembling Single-Molecule Magnets (SMMs) into coordination polymers is an area of great interest for chemists and physicists, both for the preparation of organised materials in the solid state and for the study of, and ultimately control over, the effects of inter-SMM interactions.[4]

We recently constructed a large family of oxime-based [Mn^{III}_3] and [Mn^{III}_6] complexes of general formula [$Mn^{III}_3O(R\text{-}sao)_3(L)_x(S)_y]_n$ (R = H, Me, Et, Ph; $saoH_2$ = salicylaldoxime; L = carboxylate, phosphinate, halide, perchlorate *etc*; S = ROH, H_2O, py *etc*; n =1,2) whose magnetic properties can be tuned *via* the twisting of the Mn-N-O-Mn unit (Figure 1).[5] All family members are high yielding, stable in solution and soluble in a variety of solvents. Both contain multiple terminally bonded ligands, solvent molecules and/or counter anions (depending on the reaction conditions) that can be sequentially substituted, whilst maintaining the structural integrity of the magnetic core.[6] This means that we can regard both [Mn_3] and [Mn_6] as simple molecular building blocks from which to construct novel molecule-based, potentially multifunctional, materials. Indeed we have already exploited coordination of the axial, facial acceptor sites (Figure 1, red arrows) and the equatorial donor sites (Figure 1, blue arrows) to construct families of 1-3D coordination polymers.[7]

Thus far, the moieties linking the [Mn_6] and [Mn_3] units *via* the axial acceptor sites have largely been based on carboxylate or pyridine ligands; the great advantage of both is their sheer number, diversity and ease of synthesis. Another ligand or metalloligand type which falls into this category are the cyanometallates.[8] Indeed, by combining the triangular [$Mn^{III}_3O(oxime)_3]_n$-based building blocks with cyanometalate precursors there is the potential to create hybrid materials that incorporate the advantageous physical properties of each building block, *i.e.* the tuneable SMM behaviour of the former and the predictable structure-directing effects and redox activity of the latter.[9] Given the expansive breadth of chemistry already developed for both families of compounds, such hybrid materials may offer a plethora of novel molecule-based magnets possessing interesting physical properties. Herein we present our initial foray into this field by linking [Mn^{III}_6] SMMs into 1D chains through use of the dicyanoaurate and dicyanoargentate anions [$M(CN)_2]^-$ by exploiting their linear structure-directing ability and the subsequent aurophilic and argentophilic interactions.[10]

Figure 1. (A) Schematic of the [$Mn_3O(oxime)_3]^+$ building block highlighting the red, axial acceptor sites and the blue, equatorial donor

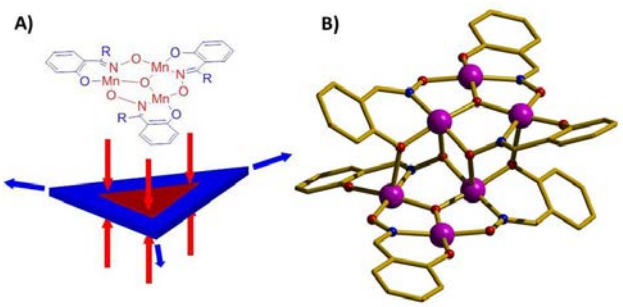

sites. (B) The [$Mn_6O_2(oxime)_6]^{2+}$ core common to the [Mn^{III}_6] family of cluster complexes, highlighting the "free" upper and lower triangular faces. Colour code: Mn = purple, O = red, N = blue.

The reaction of $Mn(NO_3)_2{\cdot}4H_2O$, Et-$saoH_2$, 3-e-py (3-ethynylpyridine), $KAu(CN)_2$ and LiOMe in MeOH results in the formation of black rod-like crystals of {[$Mn^{III}_6(\mu_3\text{-}O)_2$(Et-sao)$_6$(3-e-py)$_2$(Au(CN)$_2$)$_2$]·2MeOH}$_n$ (**1**) after slow evaporation of the filtered mother liquor after 4 days. Using $KAg(CN)_2$ and Me-$saoH_2$ in an otherwise identical reaction yields the analogous species {[$Mn_6(\mu_3\text{-}O)_2$(Me-sao)$_6$(3-e-py)$_2$(Ag(CN)$_2$)$_2$]}$_n$ (**2**; see the ESI for full details). Both crystallise in triclinic systems, with structure solution obtained in the *P*-1 space group.

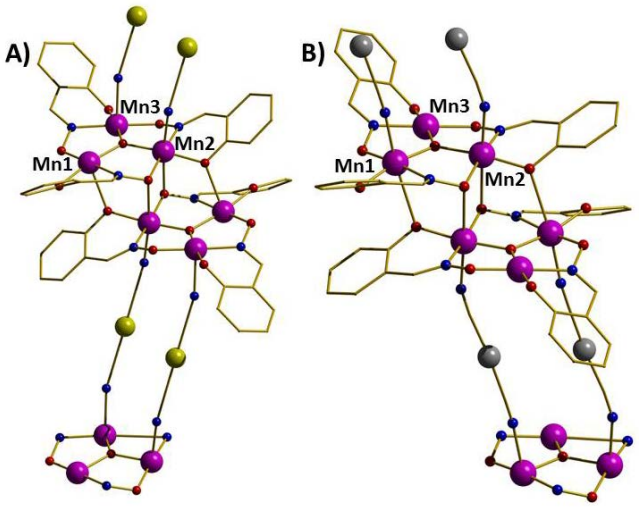

Figure 2. The structures of complexes (**1**; A) and (**2**; B). Colour code as Figure 1. Au = gold, Ag = silver. H-atoms, some C-atoms and solvent molecules have been removed for clarity.

The $\{Mn^{III}_6\}$ cores in both complexes are analogous to other members of this family[5,6] and comprise two oxo-centred triangular $[Mn^{III}_3]$ triangles linked along each edge of the triangle and between triangles through the -N-O- moiety of the oxime ligand; the latter also being mediated *via* two phenolic O-atoms. The triangular faces contain one terminally bonded 3-e-py molecule and two $[M(CN)_2]^-$ anions. Interestingly these anions are bonded to different Mn ions in **1** and **2**, as can be seen in Figure 2; Mn2 and Mn3 in the former and Mn1 and Mn2 in the latter. All Mn ions are in the 3+ oxidation state, as confirmed by a combination of bond-length considerations, BVS calculations, and charge-balance. All are six-coordinate adopting distorted octahedral geometries with their Jahn-Teller axes approximately perpendicular to the $[Mn_3]$ plane and parallel to the axis of propagation of the chain. The Mn-N-O-Mn torsion angles are 31.64°, 30.42° and 39.26°; and 34.95°, 23.78° and 36.15° for **1** and **2** respectively. The former has two angles close to (one above, one below) the 31° mark previously suggested as the tipping point between ferro- and antiferromagnetic nearest-neighbour exchange.[5,6] In general the torsions angles are smaller in **2** than in **1** reflecting the replacement of the larger Et-sao^{2-} with the smaller Me-sao^{2-}. In addition, the angles are somewhat smaller than those seen in their molecular counterparts, likely due to the "*flattening*" influence of the two $[M(CN)_2]^-$ ions and the 3-e-py ligand that sit on top of the triangular faces. The μ_3-O^{2-} which sits at the centre of this triangle lies 0.157Å and 0.073 Å above the $[Mn_3]$ plane toward the $[M(CN)_2]^-$ ions, in **1** and **2**, respectively.

There are several intra- and intermolecular H-bonding interactions: in both, the terminally bonded alcohols H-bond to phenolic and oximic O-atoms (~2.9-3.0Å), with the former also H-bonded to the MeOH solvent of crystallisation (~2.9 Å) in **1**. The closest inter-chain interaction occurs between oxime ligands with the C…C distances between neighbouring Ph and Et/Me groups of the order of 3.3-3.9 Å. The closest Mn…Mn separation in **1** is over 10 Å. In **2** the closest inter-molecular interactions occur between neighbouring 3-e-py ligands, and between the terminally bonded MeOH molecules and the Ph rings of the oxime ligands at a C…C distance of ~3.4 Å. The closest Mn…Mn separation is ~7.4 Å, somewhat shorter than that in **1**, presumably as a result of the absence of any interstitial solvent. Distances between neighbouring Au and Ag ions are ~3.6 Å, within the range expected for auro- and argentophilic interactions.[10]

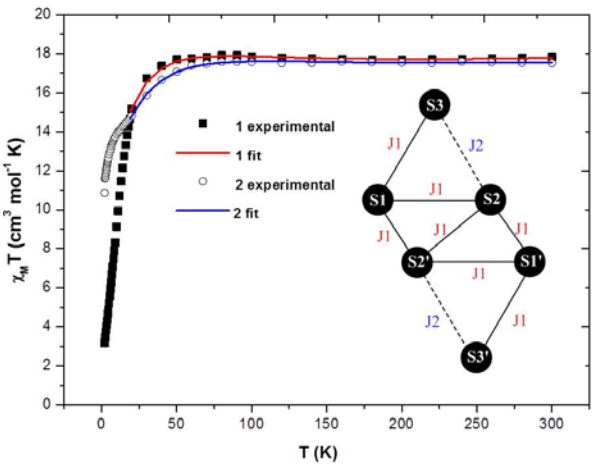

Figure 3. Plot of $\chi_M T$ *vs.* T for complexes **1** and **2** in an applied field of 0.1 T. The inset shows the coupling scheme used to fit the data to Hamiltonian (1). See text for details.

Direct current magnetic susceptibility studies were performed on polycrystalline samples of **1** and **2** in the 5–300 K range in an applied field of 0.1 T. The results are plotted as the $\chi_M T$ products *vs.* T in Fig. 3. The 300 K values of 17.8 and 17.5 cm^3 K mol^{-1} for **1** and **2** respectively are close to the spin-only value of 18 cm^3 K mol^{-1} expected for six non-interacting high-spin Mn^{III} ($3d^4$) ions with g = 2.0. For **1** the value of $\chi_M T$ remains relatively constant until ~100 K, rises slightly to a maximum value of 18.0 cm^3 K mol^{-1} at 80 K, from where it falls abruptly to a value of 3.17 cm^3 K mol^{-1} at 5 K. The value of $\chi_M T$ of **2** follows a very similar path in the high temperature (300 - 100 K) region, but deviates at lower temperatures, dropping to a small "plateau" or "shoulder" in the T = 20-10 K interval with a value between 14-15 cm^3 K mol^{-1}, before dropping more abruptly to reach a minimum value of 10.85 cm^3 K mol^{-1} at 5 K. Both behaviours are indicative of the presence of competing and weak ferro- and antiferromagnetic exchange interactions. We were able to successfully fit the data for **1** and **2** (down to T = 25 K to avoid the effects of zfs and/or any inter-molecular interactions) adopting the model schematically shown in the inset of Figure 3. The chosen coupling scheme is a reflection of the different Mn-O-N-Mn torsion angles present, in accordance with previous magneto-structural correlations for this family of complexes.[5,6] A fit of the experimental data to a Hamiltonian of the type

$$\hat{H} = -2J_1(\hat{S}_1\cdot\hat{S}_2+\hat{S}_1\cdot\hat{S}_3+\hat{S}_1\cdot\hat{S}_{2'}+\hat{S}_2\cdot\hat{S}_{2'}+\hat{S}_2\cdot\hat{S}_{1'}+\hat{S}_{1'}\cdot\hat{S}_{2'} + \hat{S}_{1'}\cdot\hat{S}_{3'}) - 2J_2(\hat{S}_2\cdot\hat{S}_3+\hat{S}_{2'}\cdot\hat{S}_{3'}) + \mu_B B g\sum_i \hat{S}_i$$

where J is the isotropic exchange interaction parameter, $\hat{S}$ is a spin-operator, i runs from 1 to 6, μ_B is the Bohr magneton, B is the applied magnetic field, g = 2 is the g-factor of the Mn^{III} ions, affords J_1 = +2.56 cm^{-1}, J_2 = -5.25 cm^{-1} for **1**, and J_1 = +2.77 cm^{-1}, J_2 = -6.17 cm^{-1} for **2**. The ground state in both cases is an S = 4,

state consistent with other family members with similar topologies.[5,6] Isothermal field-dependencies (Figure S1) are also consistent with this picture, showing a tendency to reach a saturation value of ~8 $N\mu_B$ at higher fields.

In order to investigate the possibility of interactions along the chain between different [Mn_6] moieties we performed ac susceptibility measurements in the 1.8 – 10 K temperature range with a 3.5 G ac field oscillating at frequencies up to 1284 Hz (Fig. S2). Both **1** and **2** exhibit a clear frequency-dependence in both the real and imaginary components. An Arrhenius plot constructed from the χ''_M *vs*. T data ($\tau = \tau_o \exp(U_{eff}/k_BT)$ where τ_o is the pre-exponential factor, τ is the relaxation time, U_{eff} is the barrier to the relaxation of the magnetisation and k_B is the Boltzmann constant) gave $\tau_o = 1.5 \times 10^{-10}$ s and $U_{eff} = 39.9$ K for **1**, and $\tau_o = 5.4 \times 10^{-10}$ s and $U_{eff} = 50.7$ K for **2** (Figures S3-4). The presence of *significant* intra-chain interactions between individual [Mn_6] moieties would be expected to slow down the spin dynamics at low temperatures and this would be manifested in a smaller frequency shift, k. For the experimentally accessed range of frequencies, using the average value of blocking temperature $T_B = 2.5$ and 3.4 K for **1** and **2**, respectively, the frequency shift of T_B is calculated as $k = \Delta T_B/(T_B \Delta \log f)$, where ΔT_B is the change in T_B for the frequency change $\Delta \log f = 1.7$ and 2.2 for **1** and **2**, respectively. This calculation provides the $k = 0.14$ and 0.15 for **1** and **2**, respectively, which are within the range expected for super-paramagnets and close to those reported for molecular [Mn_6] complexes. This suggests that the relaxation is in accordance with SMM behaviour, where for ideal non-interacting superparamagnets $0.1 \leq k \leq 1$,[11] and is not attributed to long range interactions mediated through the $[M(CN)_2]^-$ (M= Au, Ag) units.

Conclusions

Initial reactions combining oxime-based $[Mn_3]_n$ building blocks with cyanometalate precursors have produced chains of [Mn_6] SMMs. Their construction highlights the potential of incorporating magnetically tuneable SMM building blocks with the structure-directing effects and redox activity of Prussian Blue materials. The capacity to develop an enormous array of new materials is clear, and such hybrid materials may offer a plethora of novel molecule-based magnets possessing interesting physical properties.

Acknowledgements

We thank MINECO (MAT2012-38318-C03), the EC for a Marie Curie-IEF to GL (PIEF-GA-2011-299356) and the EPSRC.

[a]*EaStCHEM School of Chemistry, The University of Edinburgh, West Mains Road, EH9 3JJ, Edinburgh, Scotland, UK. E-mail: ebrechin@staffmail.ed.ac.uk. Tel: +44 (0)131 650 7545. Fax: +44 (0)131 650 6453.*

[b]*Instituto de Ciencia de Materiales de Aragon (ICMA), CSIC – Universidad de Zaragoza, Depto. Física Materia Condensada, 50009 Zaragoza, Spain. Email: evange@unizar.es*

[c]*UK National Crystallography Service, Chemistry, Faculty of Natural and Environmental Sciences, University of Southampton, Highfield Campus, Southampton, SO17 1BJ, UK*

†Electronic Supplementary Information (ESI) available: Experimental procedures and additional magnetic data. See DOI: 10.1039/b000000x/

Notes and references

§*Crystal data for* **1**: $C_{38}H_{39}AuMn_3N_6O_9$, M = 1086.23, triclinic, space group P-1, a = 12.9132(3), b = 13.2833(4), c = 13.3983(9) Å, α = 62.714(4), β = 76.424(5), γ = 89.144(6) °, V = 1973.96(17) Å^3, Z = 2, Absorption coefficient = 4.704 mm^{-1}, D_c = 1.828 Mg / m^3, 26779 reflections collected, 9025 unique (R_{int} = 0.0501), final R_1 = 0.0389, wR_2 = 0.0758, *GoF* = 1.045, data/restraints/parameters = 9025/0/523. Diffractometer: Single crystal X-ray diffraction data of **1** were collected on a *Rigaku AFC12* goniometer equipped with an enhanced sensitivity (HG) *Saturn724+* detector mounted at the window of an *FR-E+ SuperBright* molybdenum rotating anode generator with HF *Varimax* optics (100µm focus) S.J Coles and P.A. Gale, (2012) Chem. Sci., (3), 683-689. Cell determination and data collection: *CrystalClear-SM Expert 3.1 b18* (Rigaku, 2012). Data reduction, cell refinement and absorption correction: *CrystalClear-SM Expert 3.1 b27* (Rigaku, 2012). Structure solution and structure refinement: SHELX-2013(Sheldrick, G.M. (2008). Acta Cryst. A64, 112-122). CCDC = 976547.

Crystal data for **2**: $C_{34}H_{30}AgMn_3N_6O_8$, M = 923.33, triclinic, space group P-1, a = 12.9417(5), b = 12.9939(5), c = 14.0502(6) Å, α = 65.470(4), β = 64.209(4), γ = 60.181(4)°, V = 1784.93(15) Å^3, Z = 2, Absorption coefficient = 1.637 mm^{-1}, D_c = 1.718 g / cm^3, 29304 reflections collected, 8158 unique (R_{int} = 0.0430), final R_1 = 0.0364, wR_2 = 0.0697, *GoF* = 1.058, data/restraints/parameters = 8158/0/473. Single crystal X-ray diffraction data of **2** were collected on a Bruker ApexII CCD area detector diffractometer using monochromatized Mo-K_α radiation (λ = 0.71073 Å). CRYSALISPRO (data collection, integration and absorption correction) Agilent Technologies, (2011), *CrysAlisPro*, Agilent Technologies UK Ltd, Oxford, UK. SHELXTL (structure refinement) Sheldrick, G. M. (2008). *Acta Cryst.* A64, 112–122. SUPERFLIP (structure solution) Palatinus L. and Chapuis G. (2007). *J. Appl. Cryst.* 40, 786-790. CCDC = 976548.

1 *Making crystals by design: methods, techniques and applications*, ed. D. Braga and F. Grepioni, Wiley-VCH, Weinheim, 2007.

2 C. Janiak, *Dalton Trans.*, 2003, 2781.

3 D. Maspoch, D. Ruiz-Molina and J. Veciana, *Chem. Soc. Rev.*, 2007, **36**, 770.

4 (a) H. Miyasaka and M. Yamashita, *Dalton Trans.*, 2007, 399; (b), **122**, 163; (b) O. Roubeau and R. Clerac, *Eur. J. Inorg. Chem.*, 2008, 4325.

5 C. J. Milios, S. Piligkos and E. K. Brechin, Dalton Trans., 2008, 1809.

6 R Inglis, C. J. Milios, L. F. Jones, S. Piligkos and E. K. Brechin, *Chem. Commun.*, 2012, **48**, 181.

7 See for example: (a) C. C. Stoumpos, R. Inglis, G. Karotsis, L. F. Jones, A. Collins, S. Parsons, C. J. Milios, G. S. Papaefstathiou and E. K. Brechin, *Cryst. Growth Des.*, 2009, **9**, 24; (b) R. Inglis, A. D. Katsenis, A. Colins, F. White, C. J. Milios, G. S. Papaefstathiou and E. K. Brechin, *CrystEngComm*, 2009, **11**, 2117.

8 J.-N. Rebilly and T. Mallah, *Struct. Bonding*, 2006, **122**, 103.

9 (a) M. Nihei, Y. Sekine, N. Suganami, K. Nakazawa, A. Nakao, H. Nakao, Y.Murakami and H. Oshio, *J. Am. Chem. Soc.*, 2011, **133**, 3592; (b) V. Marvaud, C. Decroix, A. Scuiller, F. Tuyèras, C. Guyard-Duhayon, J. Vaissermann, J. Marrot, F. Gonnet and M. Verdaguer, *Chem. Eur. J.*, 2003, **9**, 1692.

10 See for example: (a) M. J. Katz, K. Sakai and D. B. Leznoff, *Chem. Soc. Rev.*, 2008, 37, 1884; (b) R. J. Roberts, X. Li, T. F. Lacey, Z. Pan, H. H. Patterson and D. B. Leznoff, *Dalton Trans.*, 2012, 41, 6992; (c) E. Colacio, F. Lloret, R. Kivekas, J. Ruiz, J. Suarez-Varela, M. R. Sundberg, *Chem. Commun.* 2002, 592.

11 L. Lecren, O. Roubeau, C. Coulon, Y.-G. Li, X. F. Le Goff, W. Wernsdorfer, H. Miyasaka and R. Clérac, *J. Am. Chem. Soc.*, 2008, 127, 17353.